

# Saturation in SPAD Indirect Time-of-Flight Imagers

François Piron and Jean-Michel Redouté

*Department of Electrical Engineering and Computer Science*

*University of Liège*

Liège, Belgium

Email: {francois.piron,jean-michel.redoute}@uliege.be

**Abstract**—Single-photon avalanche diodes (SPADs) are sensitive photodetector devices, often chosen to perform time-of-flight measurements for depth cameras because of their excellent timing properties. Indirect time-of-flight (iToF) sensors work by integrating the received signal in given time windows, then by deriving the phase from the measured photon counts. While SPAD iToF cameras give excellent results for short range measurements, they might suffer from signal deformation issues due to saturation when subjected to a high optical signal power. This saturation effect, its consequences on the signal waveform when received by the SPAD as well as on the time-of-flight distance measurements are explained and observed in this paper. A custom 0.18  $\mu\text{m}$  CMOS IC containing a SPAD iToF pixel is operated under high optical power conditions to study this effect and its repercussions. Measurements confirm that the time-of-flight accuracy will be affected if two conditions are met: the photon detection rate is close to or greater than the inverse of the dead time, and close to or greater than the signal frequency.

**Index Terms**—SPAD, time-of-flight, cw-iToF, saturation

## I. INTRODUCTION

Time-of-flight sensors rely on the duration of a photon's travel from a controlled source, towards an object and back to the sensor allowing to measure the distance with the object. When each pixel of an imager is able to measure this time-of-flight, a 3D camera is obtained.

Many time-of-flight cameras proposed in the last 20 years have been implemented using single-photon avalanche diodes (SPADs) to detect photons [1]. A SPAD is a photodiode with a reverse-bias greater than its breakdown voltage. It remains in an unstable state before eventually avalanching. When a photon hits the SPAD's active region, an avalanche might be immediately triggered with a certain probability, called photon detection probability (PDP).

SPADs are especially good photodetectors for depth imaging thanks to their single-photon sensitivity, their excellent timing precision, and their digital output allowing for in-pixel processing. Inside a time-of-flight pixel, the output of the SPAD might directly control a timer. The measurement is performed on periodic short high-power light pulses and is called direct time-of-flight (dToF). Another way of harvesting the SPAD signal to sense depth is indirect time-of-flight (iToF) [2]. Its principle is to illuminate the target with a specific periodic signal and integrate it by counting photons during

distinct time windows. The resulting count values can then be used to compute the phase or time shift between the original light modulation signal and the received one.

When an avalanche is triggered inside a SPAD, its accompanying front-end circuit will detect it, quench it by lowering the voltage across the SPAD, and finally reset the SPAD to its active state so it can detect the next photon. During this time, the SPAD will not be able to make a new detection. This is called the hold-off time or dead time (DT) and typically ranges from a few nanoseconds to hundreds of nanoseconds [3]. Therefore, at high rates of impinging photons, the SPAD might ignore incoming photons due to the dead time.

To achieve the best depth precision with iToF, as many photons as possible must be counted. There is a direct relation between phase precision  $\sigma_\varphi$  and received photon rate [4], [5]:

$$\sigma_\varphi^2 = \frac{\pi B}{8A^2}, \quad (1)$$

where  $A$  is the received signal amplitude and  $B$  is its continuous level. There are multiple factors to optimize so as to increase as much as possible the number of detected photons: illumination power, lens size, SPAD active area (related to the array fill factor), and SPAD photon detection probability (PDP) for the illumination wavelength. However, at high optical power levels, the SPAD might saturate. This kind of optical power may realistically be reached [6], [7], with large SPADs, specular reflection, focused laser sources, and/or for ranges under a few 10's of centimeters. Practically, for indirect time-of-flight sensors, SPAD saturation will affect the received signal in two ways: a reduction of its amplitude, which is mostly harmless as the amplitude is already very high, and a deformation of the signal waveform, also called pile-up distortion, which degrades the accuracy of the depth measurement.

This paper is structured as follows. Section II presents the setup used to acquire the experimental data detailed throughout the remainder of the paper. Section III discusses the saturation effect at high optical power. Section IV elaborates on its effect on the received signal waveform. Finally, time-of-flight measurements are presented and explained in Section V.

## II. EXPERIMENTAL SETUP

An abstracted diagram of the experimental setup is provided in Fig. 1. The saturation effect has been studied on a SPAD pixel implemented in a custom IC fabricated in an X-FAB

The PhD research of F. Piron was supported by a FRIA Grant funded by the FNRS, Belgium. This research is part of the Space4ReLaunch project, which is supported by the SPW Economie Emploi Recherche of the Walloon Region, under grant agreement no. 2210181.

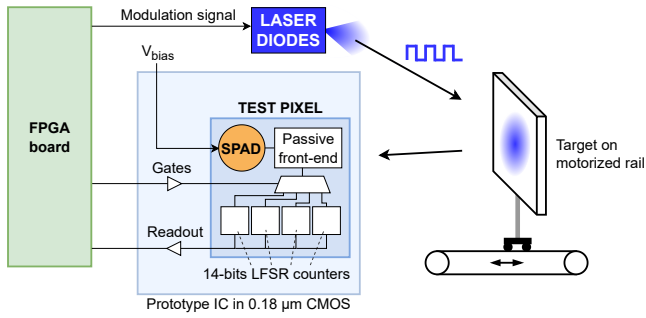


Fig. 1. Diagram of the experimental time-of-flight characterization setup.

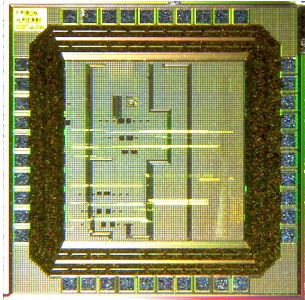


Fig. 2. Micrograph of the SPAD sensor IC fabricated in a X-FAB 180 nm CMOS process.

180 nm CMOS process, shown in Fig. 2. The IC includes several SPADs and front-end test structures. The most optimal configuration has been selected for performing the measurements presented in this work. The selected SPAD has an active area of  $11.6 \mu\text{m}^2$ . The pixel also includes a passive quenching and recharge front-end, and 14-bits linear-feedback shift register (LFSR) up/down counters for gated photon counting, controlled by external clock signals. An FPGA development board is used to generate the corresponding clock signals and for retrieving the data points.

Light is emitted from 9 laser diodes, each emitting a square wave at 450 nm with a 100 mW maximum optical power. They are unfocused, and illuminate the scene with a typical divergence of 22 degrees by 6.5 degrees. As the 9 sources are physically placed in a circle, the resulting beam is closer to a uniform circular shape. The optical rays then reach a reflective surface, mounted on a motorized rail, before coming back to the sensor. For the purpose of these experiments, external background light was blocked.

Distance is estimated using the continuous-wave iToF (cw-iToF) method, by computing the following phase estimation  $\varphi'$ , from 4 count values  $C_k$  obtained by integrating the received signal in 4 different windows with 50% duty cycle and  $\pi/2$  phase shift between each other [4]:

$$\varphi' = \text{atan} \left( \frac{C_1 - C_3}{C_0 - C_2} \right). \quad (2)$$

The phase shift is then directly linked to distance, knowing the signal frequency and the speed of light.

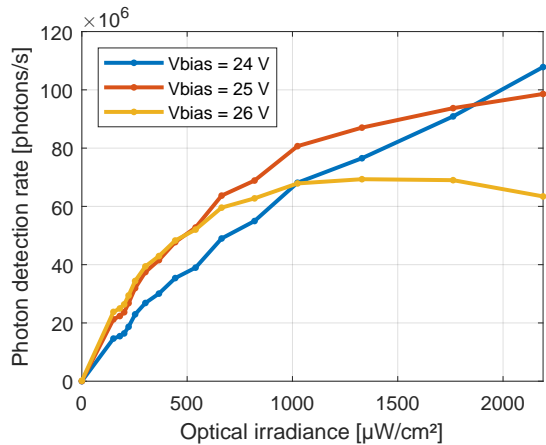


Fig. 3. Detected photons relative to incoming irradiance, for different SPAD bias voltages.

### III. SATURATION

The SPAD sensitivity can be adjusted by changing its bias voltage. But a higher sensitivity and more current through the SPAD also means an increase of the dark count rate, and of the dead time, especially with passive quenching. The theoretical maximum photon detection rate (PDR) caused by this dead time, or saturation rate, can be expressed as [8]:

$$PDR_{\text{max}} = \frac{1}{DT}. \quad (3)$$

As this paper concentrates on saturation, the afterpulsing contribution is not considered. When approaching  $PDR_{\text{max}}$ , the probability that an impinging photon is ignored because it arrives during the SPAD dead time increases, thus the effective photon detection probability decreases.

Fig. 3 shows the photon detection rate for an increasing impinging photon rate, at different SPAD bias voltages. A higher  $V_{\text{bias}}$  leads to a better PDP at low power, but also to a higher DT thus a lower saturation rate. Above a certain power level, the amount of detected photons even decreases for  $V_{\text{bias}} = 26 \text{ V}$ . This is because, due to the high bias voltage, the sensing transistor is not able to properly detect the reset of the SPAD between two photon arrivals and the output signal thus remains active for a longer period, during which no other individual photon can be counted. The value of  $PDR_{\text{max}}$  can be extracted for  $V_{\text{bias}} = 26 \text{ V}$  and is around  $70 \times 10^6$  photons/s, meaning that the dead time is around 14 ns.

### IV. SIGNAL WAVEFORM DEFORMATION

In SPAD-based iToF sensors, the shape of the detected signal has an important effect on the accuracy. If using a perfect optical sine wave, the cw-iToF estimation formula yields its exact phase [4], thus its theoretical accuracy is zero. However, when generating a high-frequency high-power optical signal, lasers and laser diodes are preferred, and only allow for a square modulation. The cw-iToF estimation will present non-linearities, and its accuracy will be mostly non-zero, with a theoretical maximum absolute value of around

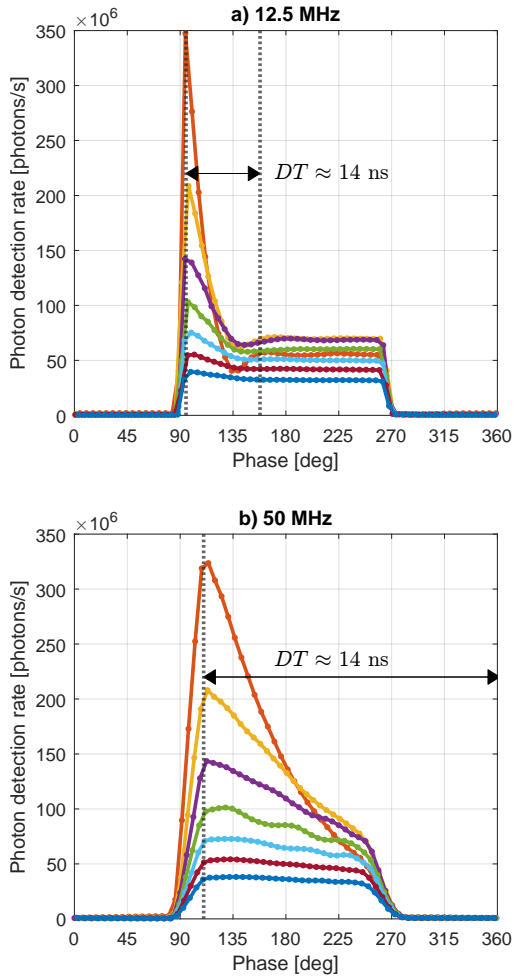


Fig. 4. Received signal waveform measured by the SPAD with  $V_{\text{bias}} = 26$  V, at different optical power levels.

1.1% of the range for an exact square wave. In practice, due to multiple jitter sources in the emitter and receiver filtering the signal, the shape of the received waveform will be between a square and a sine wave.

An optical square signal with 50% duty cycle was generated by the laser diodes at 12.5 and 50 MHz, and reflected on the target towards the SPAD sensor. The resulting waveforms are shown in Fig. 4. At the lowest irradiances, the signal is still square-shaped, albeit slightly filtered by jitter. But when the average impinging photon rate approaches saturation, a peak forms at the rising edge of the square, decays exponentially, and the detection rate during the rest of the pulse caps at  $PDR_{\text{max}}$ .

In saturation, at modulation frequencies much lower than  $PDR_{\text{max}}$ , multiple photons arrive during each signal period. The probability of a photon arriving while the SPAD is being quenched and reset from a previous detection is high. Consequently, so is the rate of ignored photons due to saturation. This phenomenon happens during the whole pulse duration, except at its beginning. The first detected photon of the pulse will always meet an active SPAD, ready to detect it. This

explains the significant peak in Fig. 4a. The slight dip just afterwards is directly correlated to this peak, as the SPAD has a higher probability of being in dead time. The amplitude of this peak corresponds to the impinging photon rate (IPR), taking into account the PDP but detected without any saturation. The time constant of the following exponential decay relates to the time it takes for the first photon of the pulse to be detected, and is thus inversely proportional to  $IPR \times PDP$ . The detection rate for the rest of the pulse is the same as for a constant illumination, as presented in Section III.

When the frequency increases, for the same impinging photon rate, the width of the peak will increase relatively to the signal's period. As there are less photons per period, each photon will have a lower probability to arrive during the SPAD dead time, thus the average detection rate will increase. If the frequency becomes so high that the dead time is longer than the width of the signal's pulse, only the peak and its exponential decay will remain. Increasing the frequency such that there is no more than a single detected photon on average per period will thus restore the original waveform shape. Note that even though the waveform stays intact in that case, the average detection rate might still be affected, if the SPAD saturates.

## V. EFFECT ON TIME-OF-FLIGHT MEASUREMENTS

When measuring time-of-flight, this signal deformation due to photon saturation will have two effects. First, as the received waveform changes and becomes asymmetric, the non-linearity error will vary and most likely increase. Second, because the received optical power might change over distance, this shape will not be constant over the whole measurement range. This will create another non-linearity error source.

In Figs. 5 and 6, the results of time-of-flight measurement under different configurations, with and without saturation, are presented. The photon detection rate and time-of-flight accuracy are compared for different optical power levels, at 12.5 MHz and 50 MHz, with a full time-of-flight non-ambiguous depth range of respectively 12 m and 3 m.

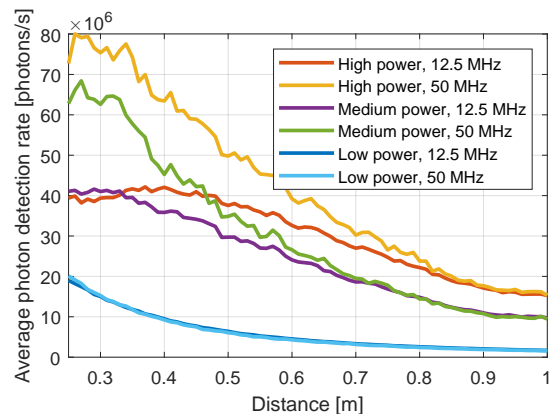


Fig. 5. Measured photon detection rate for the time-of-flight measurements presented in Fig. 6.

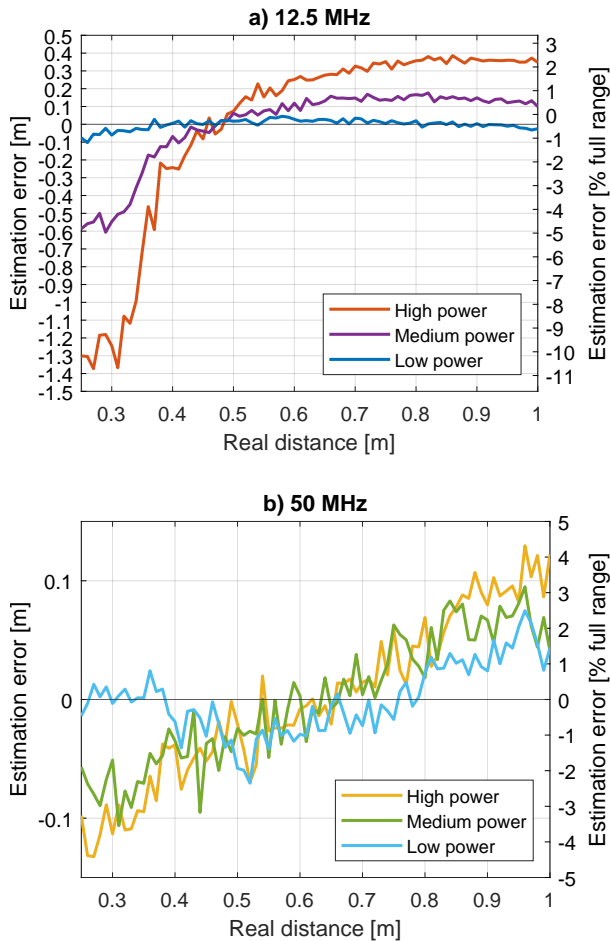


Fig. 6. Accuracy and precision of time-of-flight measurements, performed with  $V_{\text{bias}} = 26$  V.

When experiencing saturation, the accuracy is only moderately deteriorated at 50 MHz, whereas the measurements are completely unusable at lower distances at 12.5 MHz. When the signal frequency is high enough and approaches the saturation rate  $PDR_{\text{max}}$ , the first photon detection probability distribution extends over the whole period. The waveform may slightly be affected but will not suffer from significant asymmetry, and thus the cw-iToF estimation will still function adequately.

At lower frequencies, as there is a large detection peak at the beginning of the period, the induced harmonics are much stronger and depth non-linearities will ruin the accuracy. When this deformation effect is present, compensating for it using calibration to avoid the resulting non-linearity issues will be very difficult, as the error might be significant (exceeding 10% of the full range in our measurements), and its governing parameters (i.e. received optical power, PDP, and dead time) might not be constant over time. It should also be noted that even though this analysis has been performed for cw-iToF, issues of the same order are to be expected with p-iToF, as this method also depends on the signal waveform to derive distances accurately [7].

## VI. CONCLUSION

Indirect time-of-flight methods are an efficient solution for short-range depth imaging with SPADs. In this context, a high-power modulated optical emitter provides a better distance precision. However, when the impinging photon rate is too high, some photons might not be detected because of the SPAD dead time. Additionally, if the average received power is greater than one photon per signal period, a detection peak will stand out at the signal's rising edge. Because the success of indirect time-of-flight measurements depend on the received illumination signal waveform, deformation due to saturation must be avoided, by ensuring that at least one of the two following conditions are met:

$$IPR \times PDP \ll \frac{1}{DT}, \quad (4)$$

$$IPR \times PDP \ll f, \quad (5)$$

where  $IPR \times PDP$  is equivalent to the expected photon detection rate without saturation, and  $f$  is the signal's modulation frequency.

The presented experiments show that a realistic iToF sensor might encounter saturation-induced distortion in practice. Furthermore, SPADs with larger active areas, or better PDP, will be even more prone to saturation. With a passive front-end, operating the SPAD under a lower bias voltage would shorten the dead time, but at the cost of a lower PDP. Ultimately, a SPAD-based indirect time-of-flight system using a powerful modulated illumination source should favor a low SPAD dead time, and a high modulation frequency.

## REFERENCES

- [1] F. Piron, D. Morrison, M. R. Yuce, and J.-M. Redouté, "A review of single-photon avalanche diode time-of-flight imaging sensor arrays," *IEEE Sensors Journal*, vol. 21, no. 11, pp. 12 654–12 666, 2021.
- [2] C. Bamji, J. Godbaz, M. Oh, S. Mehta, A. Payne, S. Ortiz, S. Nagaraja, T. Perry, and B. Thompson, "A review of indirect time-of-flight technologies," *IEEE Transactions on Electron Devices*, vol. 69, no. 6, pp. 2779–2793, 2022.
- [3] D. P. Palubiak and M. J. Deen, "CMOS SPADs: Design issues and research challenges for detectors, circuits, and arrays," *IEEE Journal of Selected Topics in Quantum Electronics*, vol. 20, no. 6, pp. 409–426, 2014.
- [4] C. Niclass, C. Favi, T. Kluter, F. Monnier, and E. Charbon, "Single-photon synchronous detection," *IEEE Journal of Solid-State Circuits*, vol. 44, no. 7, pp. 1977–1989, 2009.
- [5] S. Donati, G. Martini, Z. Pei, and W.-H. Cheng, "Analysis of timing errors in time-of-flight LiDAR using APDs and SPADs receivers," *IEEE Journal of Quantum Electronics*, vol. 57, no. 1, pp. 1–8, 2021.
- [6] A. Kuttner, M. Hauser, H. Zimmermann, and M. Hofbauer, "Highly sensitive indirect time-of-flight distance sensor with integrated single-photon avalanche diode in 0.35  $\mu\text{m}$  CMOS," *IEEE Photonics Journal*, vol. 14, no. 4, pp. 1–6, 2022.
- [7] M. Hauser, H. Zimmermann, and M. Hofbauer, "Indirect time-of-flight with GHz correlation frequency and integrated SPAD reaching sub-100  $\mu\text{m}$  precision in 0.35  $\mu\text{m}$  CMOS," *Sensors*, vol. 23, no. 5, 2023.
- [8] D. Bronzi, F. Villa, S. Tisa, A. Tosi, and F. Zappa, "SPAD figures of merit for photon-counting, photon-timing, and imaging applications: A review," *IEEE Sensors Journal*, vol. 16, no. 1, pp. 3–12, 2016.